Journal of Integrated
SCIENCE & TECHNOLOGY

Computational insights into $FAPbI_3$ with TiO_2-ZnO as electron transport layer: A theoretical analysis

Ankit Mishra,* Manoj Kumar Nigam

Department of Electrical Engineering, MATS University, Raipur, CG, India

Received on: 02-Aug-2023, Accepted and Published on: 30-Oct-2023

Article

ABSTRACT

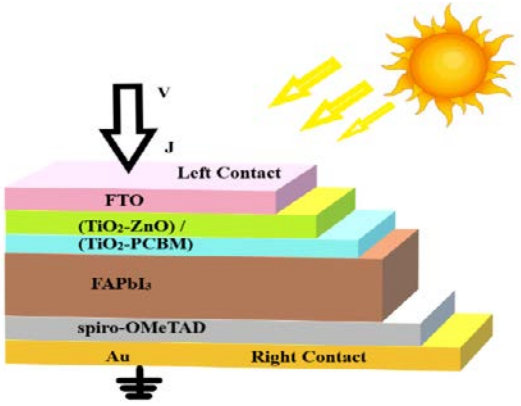

Methylammonium lead triiodide ($MAPbI_3$)-based perovskite photovoltaic cell's stability is lower than that of its formamidinium lead triiodide ($FAPbI_3$)-based counterparts. Despite this, $MAPbI_3$ solar cells offer a unique benefit regarding total power conversion efficiency (PCE). The PCE of $FAPbI_3$ solar cells was improved while maintaining their thermal stability. To determine essential parameters, the inquiry consults a variety of theoretical and experimental sources. Variations in the defect density, thickness of layers, and level of doping of the absorption layer, which is the electron transport layered (ETL), as well as the hole transportation layer (HTL) are taken into consideration, and the ideal parameters are found by a methodical examination. For the configuration FTO/TiO_2/ZnO/$FAPbI_3$/Spiro-OMeTAD/Au, the best simulation result, providing a PCE of 28%, is obtained using an open-circuit voltage (VOC), a circuit that is shorted current of 26.62 mA/cm^2, and a fill-factor (FF) of 88.5%. The suggested structure has strong thermal durability at 300 K. The effects of various transportation multiple layers affect energy band alignment, electrical field, and Recombination, and the IV properties are also thoroughly investigated.

Keywords: Perovskite, Computational Modelling, SCAPS-1D, Nanostructures, Material Science, SCAPS-1D, Nanostructures, Material Science

INTRODUCTION

Even though fossil fuel supplies are limited, the world's need for energy is now growing with every year that goes by. This demand is a key driver of global technological and economic growth. Given its ecologically advantageous characteristics that help to reduce worldwide emissions of carbon dioxide, solar cells are regarded as extremely significant sources of green power.[1] In the days to come, expectations point to a sharp increase in energy utilization. Most of today's energy comes from commencing energy sources like fossil fuels, whose supplies are soon expected to run out and which emit carbon dioxide into the atmosphere. Given the enormous need for renewable energy, creating an environmentally friendly fuel is the daunting task at hand.[2] Prices for energy are rising because of growing populations and industrialization. Due to its pure nature and absence of negative environmental effects, solar energy has been recognized as an innovation that can help with this issue. It can meet both immediate requirements and future needs. Unquestionably, the need for long-term, worldwide fuel alternatives is critical.[3] Lead perovskites composed of lead halide have been demonstrating a great deal of promise recently as capturing components for solar systems. Despite having a verified power conversion efficiency of 32.5%, lead consumption is limited because of its intrinsic toxicity, which limits its application throughout a variety of applications.[4] It has been demonstrated that the (111) facet enhances the reliability and effectiveness of PSCs in $FAPbI_3$ films. This improvement is a result of this facet's higher carrier mobility, lower exciton binding energy sources, and better stability in thermodynamics.

This limitation is the driving force for the study project, particularly looking to explore new, lead-free options in the perovskite-based material space. The tin perovskite with halide compound $CH_3NH_3SnI_3$ has recently attracted more attention due to its potential as concerning workable lead-free alternative representing use in photovoltaic technology.[5] The researchers have intensified their hypothetical and speculative investigation of the

*Corresponding Author: Ankit Mishra, Department of Electrical, MATS UNIVERSITY, Raipur, CG, India
Tel: +917224857616
Email: ankitmishra004@gmail.com

Cite as: *J. Integr. Sci. Technol., 2024, 12(2), 747.*
URN:NBN:sciencein.jist.2024.v12.747

 ISSN: 2321-4635
http://pubs.thesciencein.org/jist

material because of its relatively low band gap energies of 1.3 eV, It includes a greater percentage of the visible wavelength spectrum in contrast with different perovskite elements as well as the dangerous lead halide $CH_3NH_3PbI_3$ (band gap: 1.55 eV).[6,7] The wide 1.58 eV bandgap of $MAPbI_3$ places restrictions on the power efficiency of conversion (PCE) of PSCs constructed using this material. The use of $FAPbI_3$, which has a smaller 1.43 eV bandgap, has the potential to bring the PCE more closely to the hypothetical benchmark of more than thirty percent.[8] It has been demonstrated that the (111) facet enhances the reliability and effectiveness of PSCs in $FAPbI_3$ films. This improvement is a result of this facet's higher carrier mobility, lower exciton binding energy sources, and better stability in thermodynamics.[9] If compared to devices made using the (100) alongside (110) facets on MAPbI3 single crystals, those made on that the (110) face of MAPbBr3 one crystal showed a stunning 153% increase in responsiveness. When compared to other facets, devices using this (110) vertex with $MAPbBr_3$ showed reduced dark-current activity and increased light sensitivity, which may be explained by asymmetrical layouts and polarized discrepancies.[10]

The aforementioned (011) sides of $FAPbI_3$ are therefore predicted to exhibit admirable photovoltaic functionality, possibly enhancing the photovoltaic effectiveness with the long-term stability of PSCs. However, a substantial obstacle to uncovering their (011) sides in $FAPbI_3$ layers is the (011) plane's detrimental energetic development caused by the addition of methylammonium chloride (MACl).[11–13] Employing a variety of techniques, Researchers have attempted to increase the photovoltaic (PV) productivity of perovskite-based $MAPbI_3$ solar cells.[14–16] However, difficulties with deterioration and susceptibility to wetness have led to worries regarding device reliability.[17] When contrasted to $MAPbI_3$, however, solar cells made of perovskite constructed using formamidinium lead triiodide ($FAPbI_3$) were demonstrated to have more stable temperatures.[18] Additionally, FAPbI3 is better able to capture the sun's spectrum attributable to its energy band gap throughout 1.48 eV.[19–22] Through enabling the power source photogeneration of elec'rons (e-) besides the removal of holes (h+) through the absorption film, the charge-transfer layers, which include the layer that transports electrons (ETL) and the hole transport layer (HTL), partake a momentous influence on improving the power conversion efficiency (PCE). A comprehensive investigation of the accessible substance (HTL) and electron transportation material (ETL) in conjunction with the absorber layer is required for the enhanced performance of perovskite solar cells (PSCs). Spiro-OMeTAD stands out among the frequently used HTLs in recent research because of its organic makeup.[23] The use of zinc oxide (ZnO) using electron transportation layers (ETLs) in solar cells made from perovskite was discussed by Zhang et al. They also presented a method for producing ZnO materials. Additional studies in the same direction have shown the possibility of using ZnO as ETLs within the framework of PSCs.[24] The absorber layer, FAPbI3, has been thoroughly investigated in this work together with three other copper-based hole transporting materials (HTMs), including copper antimony sulfide ($CuSbS_2$), and carbon-based electron transport layers (ETLs), C60 and PCBM. Through numerical analysis, a comprehensive comparison is made among these three separate HTLs in terms of open-circuit voltage, power conversion efficiency, fill factor, and short-circuit current density.[25,26] When compared to the usage of C60, the analysis shows that the HTL/$CuSbS_2$ mixture with PCBM as the layer that transmits electrons produces better results. By adjusting absorbing layer depth, absorbance deficiencies concentration, Counter electrode layer (CTL) dimension, as well as doping quantities of HTL with ETL, researchers have examined how structural characteristics affect electrical responses. Finally, it has been investigated how temperature affects durability with power conversion efficiency.[27,28] These factors have been used to identify the ideal solar cell characteristics, which have significantly improved power conversion efficiency.

The internal composition underlying perovskite photovoltaic panels can be represented and improved using the SCAPS model, a software program for simulating solar cells. These solar cells are made using both organic and inorganic components, with the goal of reducing costs by switching out spiro-OMeTAD. By reducing the requirement for physical testing and expediting the experimental procedure once the ideal structure has been found, numerical simulation trials reduce the necessity for physical testing. To determine the effects of absorber layer density, electron transporter layer thickness, alongside hole transport thickness of the layers upon perovskite solar cell performance, performance assessment parameters such as open-circuit voltage (Voc), short-circuit current density (Jsc), filled factor (FF), in addition to power conversion efficiency (PCE) have been analyzed. Additionally, this study discusses the contact area frequency of the state of the defect as well as the impact of operating temperature.

EXPERIMENTAL ANALYSIS

Simulation Method and Process

The resulting related mathematical equations over semiconductors are included within the SCAPS3310 program, together with relevant boundary circumstances associated with the device's surfaces and interactions.

$$Rn,p=qnp/(\in\in o)(\mu nI+\mu pI) \quad (1)$$

$$J = qvn\mu n\varepsilon + qvp\mu p\varepsilon \quad (2)$$

$$div(\varepsilon\Delta\varphi)=- \rho \quad (3)$$

$$Jn = qvn\mu n\varepsilon + qDn\ dn/dx \quad (4)$$

$$Jp = qvp\mu p\varepsilon - qDp\ dp/dx \quad (5)$$

$$Jcond = Jn + Jp \quad (6)$$

The given equations include all necessary variables, such as the dielectric constant (Є), the foundational electronic charge (q), the generation rate (G), the recombination rate I, the diffusion coefficient (D), the potential (j), and the quantities of free holes and electrons (p and n), respectively. These equations, which frequently come up because of their nonlinear differential manifestation (Equations (1)–(3)), present tremendous obstacles to direct solutions. The complicated task of solving these equations, however, is made possible by the stipulation of distinct boundary conditions. This makes it possible to derive important device attributes, such as J-V characteristics, wavelength response actions, and capacitance-frequency and capacitance-voltage profiles.

Structure and Configuration

FTO/TiO_2/$FAPbI_3$/spiro-OMeTAD/Au makes up the basic layout, whereas we have simulated three main structures of PSC FTO/TiO_2/ZnO/$FAPbI_3$/spiro-OMeTAD/Au and FTO/ TiO_2 / PCBM / $FAPbI_3$/ spiro-OMeTAD /Au structural paradigm is introduced in conjunction with its version, FTO/TiO_2/ZnO/ $FAPbI_3$/ $CuSbS_2$/Au. The structures are simulated in the AM1.5 solar spectrum in SCAPS-1D. The temperature is set to 300k to get ideal results from the analysis.

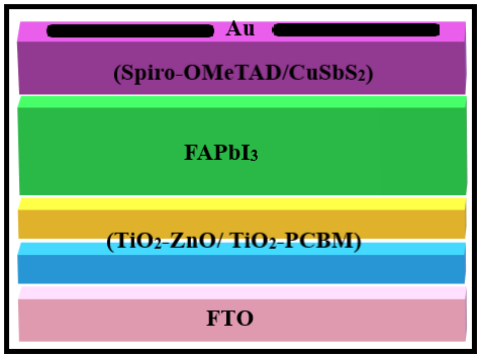

Figure 1. Configuration of perovskite solar cells used for simulations.

The three basic components of every photovoltaic system are the carrier collector, which gathers the carriers, the metal contacts, which transport the carriers to external circuitry, and the light absorber layer, which converts incident light photons into charge carriers, such as electrons and holes. Here, $MASnI_3$ and $FAPbI_3$ are the absorber materials. We have attempted to replicate the setup in a way that allows us to clearly see the effects that the input parameters are having on the device's performance characteristics. The simulation software incorporates attributes of different layers that are taken from previous research articles, with citations made to the sources of information.

Materials Parameters

Table 1: Materials Parameter SCAPS-1D Simulation

Term	FTO	TiO_2	ZnO	PCBM	$FAPbI_3$	Spiro-OMeTAD	$CuSbS_2$
Thickness (nm)	100	25	25	150	300	170	150
Eg (eV)	3.5	3.2	3.3	2	1.48	2.88	1.58
χ (eV)	4.0	4.0	4.1	4.2	4.0	2.05	4.2
Єr	9.0	100	9.0	3.9	6.6	3.00	14.6
Nc(1/cm^3)	2.2 x 10^{19}	10^{19}	4 x 10^{18}	2.5 x 10^{21}	1.2 x 10^{19}	2.2 x 10^{18}	2.0 x 10^{18}
Nv(1/cm^3)	1.8 x 10^9	10^{19}	1 x 10^{18}	2.5 x 10^{21}	2.9 x 10^{18}	1.8 x 10^{19}	1.0 x 10^{19}
μn (cm^2/Vs)	20	6x10^{-3}	100	0.2	2.7	2 x 10^{-4}	49
μp (cm^2/Vs)	10	6 x 10^{-3}	25	0.2	1.8	2 x 10-4	49
ND(1/cm^3)	2.2 x 10^{19}	10^{19}	1 x 10^{18}	2.9 x 10^{17}	1.3 x 10^{16}	1	0
NA(1/cm3)	-	-	0	0	1.3 x 10^{16}	2 x 10^{19}	1 x 10^{18}
Nt(1/cm^3)	10^{15}	10^{15}	1 x 10^{15}	10^{12}	4 x 10^{13}	10^{15}	10^{15}
Ref	21-25	24,26,27	30	28-31	32-34	35	27

Results and Discussion

Numerous facets of $FAPbI_3$ photovoltaic cells are covered in the paper. For each distinct structure, it starts by examining the energy band symmetry, electric field distribution throughout, recombination rates, and intravenous (IV characteristics. The research of modifying the absorber layer, which is the electron transportation layer (ETL), and hole transportation layer (HTL) thicknesses is then prompted by the exploration of optimum layer thicknesses. The doping levels of the charged absorber and transporting charge layers are modified once the ideal thicknesses have been established. Once the setup has reached its optimal settings, the impact of the density of defects is then seen. The research also examines how temperature variations affect how well the gadget configuration works. Spiro-OMeTAD has become an essential option for solid-state electrolytes and high-efficiency hole transport layers (HTL) in perovskite regeneration throughout the evolution of PSCs. Spiro-OMeTAD infused with Li salts is used by most high-performing PSCs to increase conductivity. Spiro-OMeTAD is often spin-coated onto PSCs during manufacture. As a result, based on spinning coating parameters the thickness of Spiro-OMeTAD was changed between 50 and 200 nm.[36] In Fig. 2, variations in acceptor density and thickness for Spiro-OMeTAD solar cells are depicted. The effect of changing the Spiro-OMeTAD layer thickness on PCE is negligible. The acceptor density of Spiro-OMeTAD may be significantly changed by experimental doping; in this work, it varied from 2 x 10^{13} to 2 x 10^{19} cm^{-3}. With rising acceptor density, PCE shows a comparable rise, peaking at roughly 26% at a density of 2 x 10^{19} cm^{-3}. This improvement is primarily supported by an increase in the fill factor (FF) and open-circuit voltage (VOC). $CuSbS_2$ has a large valence of positive band divergence of 0.27 eV, which causes it to produce a negative electric field.

In Fig. (2), the graph represents the quantum efficiency vs. wavelength (nm). The Red color graph is the standard FTO/TiO_2/$FAPbI_3$/spiro-OMeTAD/Au, the yellow color represents FTO/ TiO_2/ ZnO/ $FAPbI_3$/ $CuSbS_2$/Au with lower QE (91 %). The Blue color indicates FTO/ TiO2 / PCBM / $FAPbI_3$/ spiro-OMeTAD /Au with the 98% QE at 800 nm and the pink color represents FTO/TiO_2/ZnO /$FAPbI_3$ / spiro-OMeTAD/ Au with higher efficiency of 102% at 830 nm.

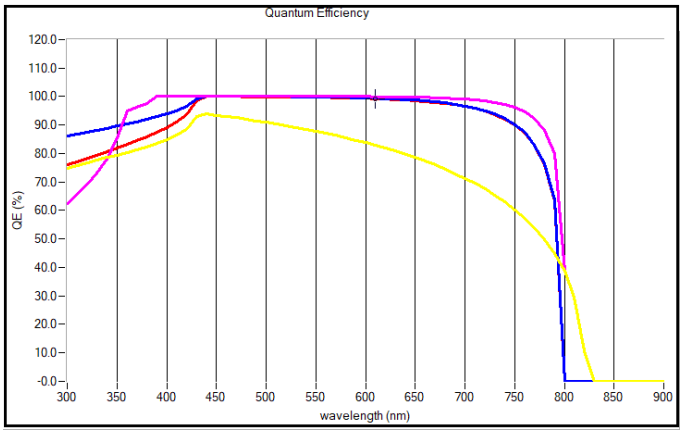

Figure 2. Quantum Efficiency Vs Wavelength (nm).

TiO_2, or titanium dioxide, along with zinc oxide (ZnO) are frequently used in layers for electron transport (ETLs) in solar cells made from perovskite (PSCs). TiO_2, which has a larger bandgap than ZnO, is less prone to light absorption, potentially reducing light loss via ETL absorption. However, compared to ZnO, TiO_2's reduced electron mobility hinders efficient electron transport.[37] On the other hand, a smaller bandgap in ZnO causes more light absorption, which can cause greater light losses. However, the greater electron mobility of ZnO increases the effectiveness of electron transport. The ideal ETL selection in PSCs is influenced by the bandgap of the perovskite material, the required efficiency, and cost concerns. Due to its ability to reduce light losses, TiO_2 is appropriate for PSCs using high bandgap perovskite materials. ZnO, on the other hand, promotes the transport of electrons in PSCs employing low bandgap perovskite materials. To make use of their complementary properties, TiO_2 and ZnO have been combined in composite ETLs or by depositing a thin film of TiO_2 on top of a larger ZnO layer. This composite ETL makes use of ZnO and TiO_2's advantages. Research conducted by Laila et al. (2018) showed that an amalgamated ETL made of ZnO and TiO_2 together functioned more efficiently 26.62% than either of the materials did on its own. The synthesis of TiO_2 and PCBM has shown the ability to produce perovskite solar cells, also called PSCs, with energy conversion efficiencies (PCE) up to 25.26%. Nevertheless, addressing current issues is necessary to improve the functioning of the gadget. The poor interaction that exists between TiO_2 & the PCBM layers and which can lead to the recombination of carriers and a decrease in efficiency, is one area of concern. Another difficulty is the existence of hysteresis, which causes the electronic device's current-voltage (I-V) graph to diverge during forward and reverse bias circumstances. Defects at the junction of the PCBM and TiO_2 layers may lead to hysteresis. Despite these challenges, it is acknowledged that the use of PCBM and TiO_2 as a layer for the transport of electrons (ETL) might be beneficial for PSCs. The goal of ongoing research is to improve these layers' properties and minimize interface flaws. The development of PSCs with higher PCEs and increased stability may result from the effective deployment of upgrades.

The performance in a PSC (Perovskite Photovoltaic Cell) is greatly influenced by the right arrangement of the energy bands connecting the charge transport elements (HTL & ETL) & and the perovskite material. A close alignment of the conductivity band in the ETL and PSC is necessary to provide optimum electron detachment from the perovskite substance while reducing any offset. For their valence bands, however, an immense offset is preferred. By preventing undesirable hole transfer from reaching the ETL, this difference in valence band locations helps avoid recombination events. Conversely, a significant valence band offset between the HTL as well as PSC is desirable for efficient hole harvesting within the crystalline substance. Their conductor bands have to be barely aligned at the same time.

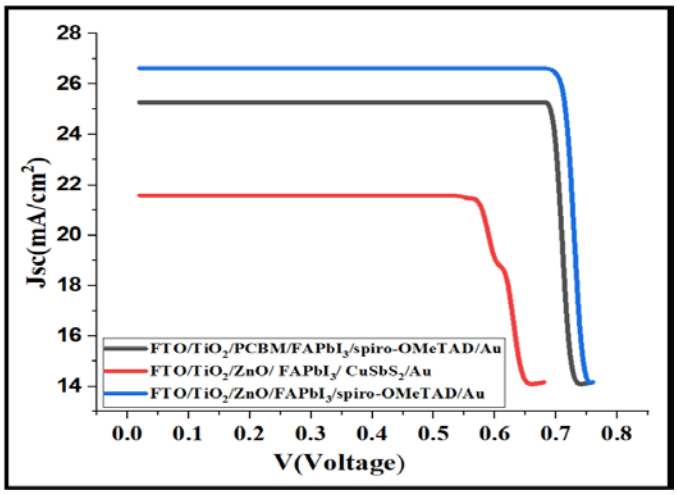

Figure 3. IV Characteristics of Solar Cell

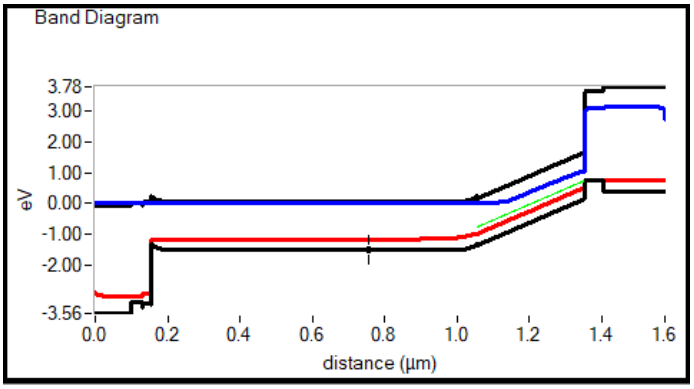

Figure 4. Band Diagram of FTO/TiO_2/ZnO/ $FAPbI_3$/ spiro-OMeTAD/Au

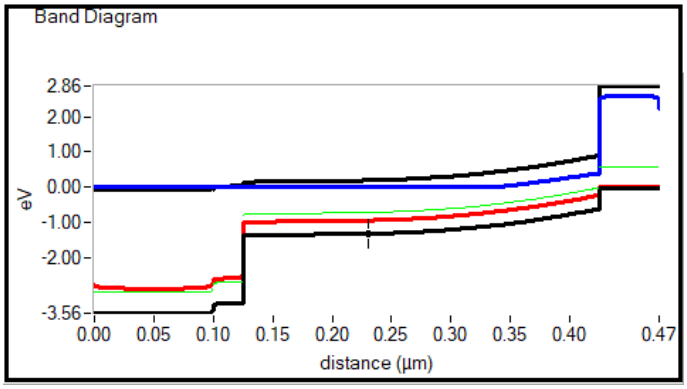

Figure 5. Band Diagram of FTO/TiO_2/PCBM/ $FAPbI_3$/ spiro-OMeTAD/Au

In Fig. (4), the $FAPbI_3$ shows the immense rise in the Bandgap associated with TiO_2-ZnO ETL materials. The change in eV is from -3.56 eV to 3.78 eV, which shows the high-rate charge transfer in PCE.

The Jsc (mA/cm^2) of TiO_2-PCBM/ $FAPbI_3$ is 21. 1%. The ETL energy band compatibility & and the perovskite crystal result in minor conductivity band offsets in the two materials.

The overall eV in Figure 5, is less than Figure 4. The eV generated here is from -3.56 to 2.86. The absorption energy of TiO_2-PCBM/ $FAPbI_3$ is very low as compared to TiO_2-ZnO/ $FAPbI_3$.

CONCLUSIONS

The examination of formamidinium lead triiodide ($FAPbI_3$) in three different configurations—TiO_2-ZnO/$FAPbI_3$/spiro-OMeTAD, TiO_2-PCBM/$FAPbI_3$/$CuSbS_2$—is the focus of this work. Each charge transporting layer (CTL) and the $FAPbI_3$ absorber layer are independently examined as part of the inquiry using SCAPS 1-D simulation software. This strategy seeks to identify the best settings for each layer. The study identifies the suitable thickness along with the doping concentration of each layer inside various architectures through a thorough, methodical examination. The outcomes highlight the fact that using these adjusted settings produces the best cell output performance. The most effective design, with a PCE, or power conversion efficiency, of 28%, is the TiO_2-ZnO/$FAPbI_3$/spiro-OMeTAD one. The impressive current density (JSC) of this structure is 26.62 mA/cm^2, the open-circuit voltage (VOC) is 0.76 V, and the fill factor (FF) is 88.5%. The amount of material and defect density associated with the $FAPbI_3$ perovskite absorbing layer are crucial variables influencing PCE and other solar cell characteristics, according to the study's comprehensive assessment of the impact of each of the layers on photovoltaic performance. It's interesting to note that neither the expensive organic spiro-OMeTAD nor the affordable inorganic $CuSbS_2$ significantly affect the thickness overall acceptor density of PSCs. Furthermore, PCE in PSCs is very little impacted by the donor density and thickness of FTO and TiO_2.

ACKNOWLEDGMENTS

Author (AM) acknowledge Marc Burgelman for providing with the SCAPS-1D.

CONFLICT OF INTEREST STATEMENT

There is no conflict of Interest.

REFERENCES

1. E. González-Juárez, A. Espinosa-Roa, A.T. Cadillo-Martínez, et al. Enhancing the stability and efficiency of MAPbI3 perovskite solar cells by theophylline-BF4− alkaloid derivatives, a theoretical-experimental approach. *RSC Adv.* **2023**, 13 (8), 5070–5080.
2. W. Qiu, Y. Wu, Y. Wang, et al. Low-Temperature robust MAPbI3 perovskite solar cells with power conversion efficiency exceeding 22.4%. *Chem. Eng. J.* **2023**, 468.
3. G. Nasti, A. Abate. Tin Halide Perovskite (ASnX3) Solar Cells: A Comprehensive Guide toward the Highest Power Conversion Efficiency. *Adv. Energy Mater.* **2020**, 10 (13), 1902467.
4. S. Weber, T. Rath, B. Kunert, et al. Dependence of material properties and photovoltaic performance of triple cation tin perovskites on the iodide to bromide ratio. *Monatshefte fur Chemie* **2019**, 150 (11), 1921–1927.
5. H.J. Du, W.C. Wang, J.Z. Zhu. Device simulation of lead-free CH3NH3SnI3 perovskite solar cells with high efficiency. *Chinese Phys. B* **2016**, 25 (10), 108802.
6. Q.Y. Chen, Y. Huang, P.R. Huang, et al. Electronegativity explanation on the efficiency-enhancing mechanism of the hybrid inorganic-organic perovskite ABX3 from first-principles study. *Chinese Phys. B* **2015**, 25 (2), 027104 1–6.
7. Umari, P.; Mosconi, E. and De Angelis, F. Relativistic GW calculations on CH3NH3PbI3 and CH3NH3SnI3 perovskite for solar cells applications,. *Sci. Rep.* **2014**, 4, 4467.
8. H. Min, D.Y. Lee, J. Kim, et al. Perovskite solar cells with atomically coherent interlayers on SnO2 electrodes. *Nature* **2021**, 598 (7881), 444–450.
9. C. Ma, M. Grätzel, N.G. Park. Facet Engineering for Stable, Efficient Perovskite Solar Cells. *ACS Energy Lett.* **2022**, 7 (9), 3120–3128.
10. Z. Zuo, J. Ding, Y. Zhao, et al. Enhanced Optoelectronic Performance on the (110) Lattice Plane of an MAPbBr3 Single Crystal. *J. Phys. Chem. Lett.* **2017**, 8 (3), 684–689.
11. J. Ding, B. Liu, X. Zhan, et al. Low defect density and anisotropic charge transport enhanced photo response in pseudo-cubic morphology of MAPbI3 single crystals. *ACS Appl. Energy Mater.* **2020**, 3 (11), 10525–10532.
12. Z. Xu, Z. Liu, N. Li, et al. A Thermodynamically Favored Crystal Orientation in Mixed Formamidinium/Methylammonium Perovskite for Efficient Solar Cells. *Adv. Mater.* **2019**, 31 (24), 1900390.
13. M. Kim, G.H. Kim, T.K. Lee, et al. Methylammonium Chloride Induces Intermediate Phase Stabilization for Efficient Perovskite Solar Cells. *Joule* **2019**, 3 (9), 2179–2192.
14. S.A. Moyez, S. Roy. Dual-step thermal engineering technique: A new approach for fabrication of efficient CH3NH3PbI3-based perovskite solar cell in open air condition. *Sol. Energy Mater. Sol. Cells* **2018**, 185, 145–152.
15. M.S. Jamal, S.A. Shahahmadi, P. Chelvanathan, et al. Effect of defect density and energy level mismatch on the performance of perovskite solar cells by numerical simulation. *Optik (Stuttg).* **2019**, 182, 1204–1210.
16. S. Rai, B.K. Pandey, D.K. Dwivedi. Modeling of highly efficient and low cost CH3NH3Pb(I1-xClx)3 based perovskite solar cell by numerical simulation. *Opt. Mater. (Amst).* **2020**, 100, 109631.
17. A.K. Jena, A. Kulkarni, T. Miyasaka. Halide Perovskite Photovoltaics: Background, Status, and Future Prospects. *Chem. Rev.* **2019**, 119 (5), 3036–3103.
18. M.B. Kanoun, A.A. Kanoun, A.E. Merad, S. Goumri-Said. Device design optimization with interface engineering for highly efficient mixed cations and halides perovskite solar cells. *Results Phys.* **2021**, 20, 103707.
19. R. Pandey, R. Chaujar. Technology computer aided design of 29.5% efficient perovskite/interdigitated back contact silicon heterojunction mechanically stacked tandem solar cell for energy-efficient applications. *J. Photonics Energy* **2017**, 7 (2), 022503.
20. Q. Han, S.H. Bae, P. Sun, et al. Single Crystal Formamidinium Lead Iodide (FAPbI3): Insight into the Structural, Optical, and Electrical Properties. *Adv. Mater.* **2016**, 28 (11), 2253–2258.
21. S. Wozny, M. Yang, A.M. Nardes, et al. Controlled Humidity Study on the Formation of Higher Efficiency Formamidinium Lead Triiodide-Based Solar Cells. *Chem. Mater.* **2015**, 27 (13), 4814–4820.
22. G.E. Eperon, S.D. Stranks, C. Menelaou, et al. Formamidinium lead trihalide: A broadly tunable perovskite for efficient planar heterojunction solar cells. *Energy Environ. Sci.* **2014**, 7 (3), 982–988.
23. D. Wang, M. Wright, N.K. Elumalai, A. Uddin. Stability of perovskite solar cells. *Sol. Energy Mater. Sol. Cells* **2016**, 147, 255–275.
24. P. Zhang, J. Wu, T. Zhang, et al. Perovskite Solar Cells with ZnO Electron-Transporting Materials. *Adv. Mater.* **2018**, 30 (3), 1703737.
25. D.Y. Son, J.H. Im, H.S. Kim, N.G. Park. 11% efficient perovskite solar cell based on ZnO nanorods: An effective charge collection system. *J. Phys. Chem. C* **2014**, 118 (30), 16567–16573.
26. Z.L. Tseng, C.H. Chiang, C.G. Wu. Surface Engineering of ZnO Thin Film for High Efficiency Planar Perovskite Solar Cells. *Sci. Rep.* **2015**, 5, 13211.
27. G. Liu, Y. Zhong, H. Mao, et al. Highly efficient and stable ZnO-based MA-free perovskite solar cells via overcoming interfacial mismatch and deprotonation reaction. *Chem. Eng. J.* **2022**, 431, 134235.

28. X. Wu, J. Zhang, M. Qin, et al. ZnO electron transporting layer engineering realized over 20% efficiency and over 1.28 V open-circuit voltage in all-inorganic perovskite solar cells. *EcoMat* **2022**, 4 (4), 12192.
29. S.P. Ong, W.D. Richards, A. Jain, et al. Python Materials Genomics (pymatgen): A robust, open-source python library for materials analysis. *Comput. Mater. Sci.* **2013**, 68, 314–319.
30. L. Ward, A. Dunn, A. Faghaninia, et al. Matminer: An open source toolkit for materials data mining. *Comput. Mater. Sci.* **2018**, 152, 60–69.
31. D.K. Barupal, O. Fiehn. Generating the blood exposome database using a comprehensive text mining and database fusion approach. *Environ. Health Perspect.* **2019**, 127 (9), 2825–2830.
32. W. McKinney. Data Structures for Statistical Computing in Python. In *Proceedings of the 9th Python in Science Conference*; Austin, TX, USA, **2010**; Vol. 445, pp 56–61.
33. Z. Jin, J. Shang, Q. Zhu, et al. RFRSF: Employee Turnover Prediction Based on Random Forests and Survival Analysis. In *Lecture Notes in Computer Science (including subseries Lecture Notes in Artificial Intelligence and Lecture Notes in Bioinformatics)*; Springer, Berlin/Heidelberg, Germany, **2020**; Vol. 12343 LNCS, pp 503–515.
34. T. Bendib, H. Bencherif, M.A. Abdi, et al. Combined optical-electrical modeling of perovskite solar cell with an optimized design. *Opt. Mater. (Amst).* **2020**, 109, 110259.
35. Y. Zhang, S. Seo, S.Y. Lim, et al. Achieving Reproducible and High-Efficiency (>21%) Perovskite Solar Cells with a Presynthesized FAPbI3 Powder. *ACS Energy Lett.* **2020**, 5, 360–366.
36. C.V. Rudrappa, S. Ganesan. Investigation of performance and stability of multilayered organometallic halide Perovskite cell. *J. Integr. Sci. Technol.* **2023**, 11 (1), 465.
37. M.V. Bhute, Y.P. Mahant, S.B. Kondawar. Titanium dioxide / poly(vinylidene fluoride) hybrid polymer composite nanofibers as potential separator for lithium ion battery. *J. Mater. Nanosci.* **2017**, 4 (1), 6–12.